Nanoscale

PAPER

Promote potential applications of nanoparticles as respiratory drug carrier: insights from molecular dynamics simulations†

Xubo Lin,[a] Tingting Bai,[a] Yi Y. Zuo[b] and Ning Gu*[a]

Nanoparticles (NPs) show great promises in biomedical applications as the respiratory drug carrier system. Once reaching the alveolar region, NPs first interact with the pulmonary surfactant (PS) film, which serves as the first biological barrier and plays an important role in maintaining the normal respiratory mechanics. Therefore, understanding the interactions between NPs and PS can help promote the NP-based respiratory drug carrier systems. Using coarse-grained molecular dynamics simulations, we studied the effect of rigid spherical NPs with different hydrophobicity and sizes on a dipalmitoylphosphatidylcholine (DPPC) monolayer at the air–water interface. Four different NPs were considered, including hydrophilic and hydrophobic NPs, each with two diameters of 3 nm and 5 nm (the sizes are comparable to that of generation 3 and 5 PAMAM dendrimers, which have been widely used for nanoscale drug carrier systems). Our simulations showed that hydrophilic NPs can readily penetrate into the aqueous phase with little or no disturbance on the DPPC monolayer. However, hydrophobic NPs tend to induce large structural disruptions, thus inhibiting the normal phase transition of the DPPC monolayer upon film compression. Our simulations also showed that this inhibitory effect of hydrophobic NPs can be mitigated through PEGylation. Our results provide useful guidelines for molecular design of NPs as carrier systems for pulmonary drug delivery.

Introduction

Nanoparticles (NPs) have received intense interests for their advantages in broad biomedical applications such as drug delivery, bio-imaging, bio-sensing, specific targeting, *etc.*[1–6] For example, there have been extensive studies on the applications of NPs in respiratory therapeutics.[7–11] The human lungs are easily accessible due to its large surface area, thin epithelial barrier, abundant underlying vasculature, low proteolytic activity, low acidity and thin mucus layer. NPs as drug carriers have been shown to improve drug stability, bioavailability, targeting, uptake and biological activity. Hence, using inhaled nanoparticles as drug carriers to the respiratory system shows great promises for treating lung diseases.

As mentioned above, NPs have easy access to the respiratory system. Thus, one of the key scientific issues in the applications of NPs as drug carriers in respiratory therapeutics is the balance between the penetration ability across the alveolar barrier and the relative side effects of the NPs.[12,13] In the present work, attention is focused on pulmonary surfactant (PS), which lines the entire alveolar surface and serves as the first biological barrier for particle translocation after inhalation. PS maintains normal respiratory mechanics by reducing alveolar surface tension at the air–liquid interface and thus prevents the lung from collapsing at the end of expiration.[14] PS consists of approximately 90% lipids, with dipalmitoylphosphatidylcholine (DPPC) being the most abundant single lipid component for most mammalian species, and 10% proteins. Both experiments[14–18] and computer simulations[19–21] have confirmed that the phospholipids of PS undergo surface phase transition during the respiratory cycles. During the expiration process (*i.e.*, film compression), phospholipid monolayers undergo surface phase transitions from a "fluid-like" liquid-expanded (LE) phase to a "solid-like" liquid-condensed (LC) phase, which is opposite to the direction of phase transition in the inspiration process (*i.e.*, film expansion). Phospholipid phase transition and separation have been proven to play an important role in regulating the biophysical function of PS film.[14,17] When the lateral structure of the PS film is disrupted, lipid molecules may detach from the air–water interface, which affects PS homeostasis.[22]

In this work we used coarse-grained (CG) molecular dynamics simulations to probe the effects of NPs of different hydrophobicity and sizes on DPPC monolayers during the

[a]State Key Laboratory of Bioelectronics and Jiangsu key Laboratory for Biomaterials and Devices, School of Biological Science & Medical Engineering, Southeast University, Nanjing, 210096, People's Republic of China. E-mail: guning@seu.edu.cn; Fax: +86-25-83272460; Tel: +86-25-83272476

[b]Department of Mechanical Engineering, University of Hawaii at Manoa, Honolulu, Hawaii 96822, USA

† Electronic supplementary information (ESI) available. See DOI: 10.1039/c3nr04163h

compression and expansion process (see Fig. 1 for simulation setup). DPPC is the major component of PS responsible for surface tension reduction.[14,19–28] Hence, our simulations may provide useful insights into promoting NP-based pulmonary drug delivery.

The rest of this work is organized as follows: section 2 describes the model and the simulation details. In section 3, four NPs will be considered: hydrophobic NP (diameter d = 3 nm, 5 nm) and hydrophilic NP (d = 3 nm, 5 nm). The respiratory cycle consists of two main processes: the compression process and the expansion process. Hence, we will study the interactions of NPs with the DPPC monolayer at the air–water interface during both the compression process and the expansion process, respectively. Structural disruptions by NPs and the effects on phase transition dynamics of the DPPC monolayer will be analyzed. Section 4 summarizes our main findings and concludes the paper.

Simulation methods

Coarse-grained model

Compared to atomistic models, coarse-grained (CG) models, which map several atoms into one interaction site and have near-atomic resolution, allow simulations to be performed with a longer time period and a larger length scale.[29–32] Martini force field is one of the most popular coarse-grained models,[29,30] which has been widely used to simulate biomolecules, such as lipids, *etc.* and is open to be used for NPs.

Martini CG model is based on a four-to-one mapping, *i.e.*, on average four heavy atoms are represented by a single interaction

center. Only four main types of interaction sites: polar (P), nonpolar (N), apolar (C), and charged (Q). Each particle type has a number of subtypes, which allow for a more accurate representation of the chemical nature of the underlying atomic structure. Within a main type, subtypes are either distinguished by a letter denoting the hydrogen-bonding capabilities (d donor, a acceptor, da both, 0 none), or by a number indicating the degree of polarity (from 1, low polarity, to 5, high polarity). A shifted Lennard-Jones (LJ) 12-6 potential energy function and a shifted coulombic potential energy function are used to describe the non-bonded interactions. A weak harmonic potential is applied for the bonded interactions. More details can be found in the paper of Marrink *et al.*[29]

The CG DPPC and water force field parameters were given in details by Marrink *et al.*[29] and downloaded from http://md.chem.rug.nl/cgmartini/. For the CG spherical NPs, we used only one bead type to stack relative NP, Nda-type for hydrophilic NP and C1-type for hydrophobic NP (Nda and C1 are parameters in Martini force field).[29] Spherical NP was stacked by beads that were evenly spaced on the surfaces of concentric spheres. Beads within 1 nm were constrained by a spring to confirm rigid NPs as reported by our previous work.[33] In total, four different kinds of NPs were constructed with two sizes (d = 3 nm, 5 nm) and hydrophobic/hydrophilic properties.

Simulation details

As shown in Fig. 1, we used the bi-monolayer system, which has been validated by many researchers,[19–21,28] to probe the interactions between inhaled NPs and DPPC monolayer. The air space was represented by vacuum and PS was modeled by a pure DPPC monolayer. Our bi-monolayer system consisted of 2 × 1024 DPPC molecules and 82944 CG water molecules. The normal of these two monolayers was set as the z-axis of the simulation system. After performing compression and expansion simulations, we extracted two frames from the resulting trajectories: one (averaged area per lipid A_{av} = 0.64 nm², LE phase according to ref. 16, box: 25.58 nm × 25.58 nm × 40 nm) as the initial conformation of the compression simulations for NP–DPPC monolayer systems; the other one (A_{av} = 0.47 nm², LC phase according to ref. 16, box: 22.01 nm × 22.01 nm × 40 nm) as the initial conformation of the expansion simulations. NPs were placed in the vacuum of these two frames near the DPPC monolayer separately to mimic the state of NP's deposition onto the PS film from the air space, followed by the compression and expansion simulations. For each of these simulations, time scale as long as 2.0 μs was performed. As we know, the time scale of respiration may be many orders of magnitude longer than μs. It is still rather difficult to perform so longer time scale using CG model. Hence, larger lateral pressures are often used for simulations in order to reproduce the normal phase transition process of the interfacial lipid molecules on μs time scale.[19–21] Besides, we systematically study the system of NP : DPPC = 1 : 1024 (a relative high ratio) and do not focus on the concentration effects of NPs on the DPPC monolayer at the present work. So, these treatments should be considered for
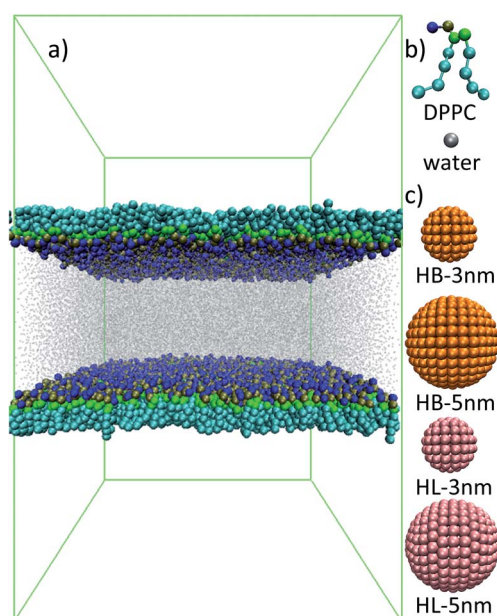

Fig. 1 (a) System setup, (b) lipid, water and (c) nanoparticles in the MARTINI model. Color scheme: head-groups of DPPC in blue-tan-green, tail of DPPC in cyan, water in silver, hydrophobic NP (HB) in orange, hydrophilic NP (HL) in pink, simulation box edges in lime. Nanoparticles are named as HB-diameter or HL-diameter.

insights from the simulation results for designing nano-particles as respiratory drug carriers.

For all simulations, a cutoff of 1.2 nm was used for van der Waals (vdW) interactions, and the Lennard-Jones potential was smoothly shifted to zero between 0.9 nm and 1.2 nm to reduce cutoff noise. For electrostatic interactions, the coulombic potential, with a cutoff of 1.2 nm, was smoothly shifted to zero from 0 to 1.2 nm. The relative dielectric constant was 15, which was the default value of the force field.[29] Lipids, water and NPs were coupled separately to Berendsen heat baths[34] at $T = 310$ K, with a coupling constant $\tau = 1$ ps. The monolayer compression was simulated using semiisotropic pressure coupling (Berendsen coupling scheme,[34] coupling constant of 4 ps, compressibility in the lateral direction of 5×10^{-5} bar^{-1} and in the normal direction of zero). Each of the simulations were performed for 2.0 μs with a time step of 20 fs. The neighbor list for non-bonded interactions was updated every 10 steps. Snapshots of the simulation system in this paper were all rendered by VMD.[35] All simulations were performed with the GROMACS simulation package.[36]

Two-dimensional phase map

Order parameter of the lipid's tail can represents the molecular orientation of the tail and can be calculated using the formula

$$ S_{z,n} = \left\langle \frac{1}{2} \left(3 \cos^2 \theta_n - 1 \right) \right\rangle $$

where θ_n is the angle between the vector connecting the $n-1$ and $n+1$ sites of the tail and the monolayer normal z.

DPPC monolayers at the LE, the LC–LE coexistence, and the LC phases have different order degrees of molecular orientations, which can be characterized by molecular imaging of monolayer thickness in experiments[14,18,37] or computing the order parameter in simulations.[21,28] We have developed a two-dimensional (2D) phase map method to display the detailed phase behaviors of the DPPC monolayer.[28] In 2D phase map, each point represents the center-of-mass (COM) of an interfacial DPPC molecule and is colored according to the order parameter of this molecule, thus mapping the molecular orientations of interfacial monolayers. These 2D phase maps show perfect consistency with monolayer thickness as shown in the ESI (Fig. S1†).

Results and discussion

Monolayer penetrations and structural disruptions caused by NPs

To understand the effects of hydrophobicity/hydrophilicity and size of NPs on monolayer penetrations and structural disruptions, we first show the time evolution of the simulation system (Fig. 2). As shown in Fig. 2, we considered both the compression and expansion processes. We found that the hydrophobic NP tends to cause large structural disruptions of DPPC monolayer and form DPPC-coated NP structure during the compression process, which is consistent with the case of large fullerene nanoparticles reported by Chiu et al.[38] And the structure of smaller hydrophobic NP ($d = 3$ nm, HB-3 nm) immerges into the water phase deeper than that of hydrophobic NP ($d = 5$ nm, HB-5 nm). We did not observe that this DPPC-coated NP structure detaches from the DPPC monolayer completely in our compression simulations. This structural disruption disappeared in the next expansion simulations returning to the initial state (data not shown). During the expansion process, hydrophobic NPs just embed themselves in the hydrophobic tails of the DPPC molecules and show little impacts on the DPPC monolayer. In other words, hydrophobic NPs penetrate DPPC monolayer neither in compression process nor in expansion process.

Hydrophilic NP behaves quite differently from the hydrophobic NP. Hydrophilic NP can easily penetrate the DPPC monolayer in the compression process and nearly cross the DPPC monolayer during the expansion process (Fig. 2). Little or no structural disruptions appear. Considering the good monolayer penetration ability and little structural disruptions, our simulations suggests that hydrophilic NPs may serve as a potential carrier for respiratory drug delivery.

As discussed above, hydrophobicity and hydrophilicity of NPs show an significant differences in monolayer penetration ability and relative structural disruptions. This is because that it is energy-favorable for hydrophobic NP to interact with the hydrophobic tails of DPPC molecules and for hydrophilic NP to interact with the hydrophilic head-groups of DPPC molecules and water molecules,[29,30,33,38] which modulates the interaction dynamics between NP and the DPPC monolayer. Besides, the disruption structure caused by the smaller hydrophobic NP (HB-3 nm) can immerge into the water phase deeper than that structure caused by HB-5 nm. The smaller hydrophobic NP corresponds to smaller increase of the in-plane rigidity of the DPPC monolayer in this same concentration, which explains the size effects of NPs on structural disruptions of the monolayer.[39]

NP-induced phase behavior change of DPPC monolayer

DPPC molecules of different phases correspond to different molecular arrangements, which regulate the role of the DPPC monolayer in reducing the surface tension of the air–water interface and in the gas-exchange process.[16–21] During the compression process, the interfacial molecules of pure DPPC monolayer change from the LE phase to LC–LE coexistence and then to the LC phase, indicated by the increase of the order parameter of the DPPC molecules (Fig. S1† and 3); the reverse process takes place upon film expansion (Fig. S1† and 3), which is defined as normal phase transition.[28] Here, the interfacial DPPC molecules refer to the DPPC molecules that remain at the air–water interface and don't include the DPPC molecules from NP-induced disruption structures (Fig. S2†). For all simulations, NPs show little or no influence on the normal phase transition of interfacial DPPC molecules during the expansion process. And only hydrophobic NPs (B-3 nm, B-5 nm) tend to inhibit the normal phase transition of interfacial DPPC molecules during the compression process.
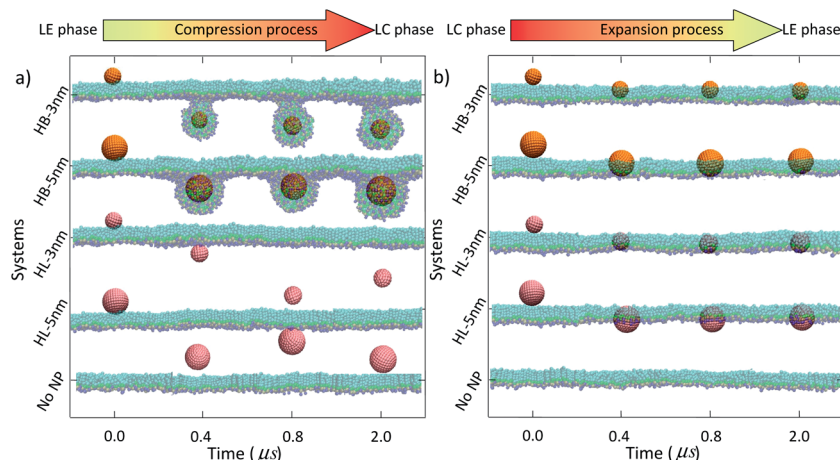
Fig. 2 Structural disruptions by NPs and monolayer penetration ability of NPs both in compression (a) and expansion (b) processes. It is found that hydrophobic NP tends to induce large structural disruptions during compression process, while hydrophilic NP is easy to penetrate DPPC monolayer with little or no disruptions to DPPC monolayer. All NPs show little influences on the DPPC monolayer during the expansion process. The color for DPPC and NPs are the same as Fig. 1. And water molecules are not shown for clarity.

As shown in Fig. 3, both the compression and expansion simulations reach the equilibrium states after approximately 0.4 μs. To obtain more information about how NP inhibited the normal phase transition of DPPC monolayer, the two-dimensional (2D) phase maps of the interfacial DPPC molecules and top-view snapshots of the systems (at $t = 0.8$ μs) during the compression and the expansion processes are shown in Fig. 4. The points of the map represent the interfacial DPPC molecules and the blank regions of the map correspond to the situations that the large structural disruption is induced by NPs or the DPPC monolayer is embedded with NPs (Fig. 4 and S2†). Both the phase maps and snapshots validate that only hydrophobic NPs can inhibit the normal phase transition of interfacial DPPC molecules during the compression process. Besides, we choose an equilibrium state ($t = 0.8$ μs) to perform NVT simulations, in

order to calculate the surface tension of the DPPC monolayer. The results show both hydrophobic NPs and hydrophilic NPs have little effects on the surface tension of the DPPC monolayer (Fig. S3†). Our simulation results are consistent with the experimental results reported by Tatur et al.,[40] whose experiments point out that hydrophobic NPs do not influence the π–A isotherm, but do alter the nucleation, growth, and morphology of the condensed domains in the DPPC monolayer.

On one hand, large structural disruptions of DPPC monolayer can make some DPPC molecules detach from the air–water interface, which may further affect PS homeostasis.[22] On the other hand, the normal phase transition of interfacial DPPC molecules plays an important role in regulating the mechanics of air–water interface and the inhibition of this normal phase transition may disturb the regulation of the
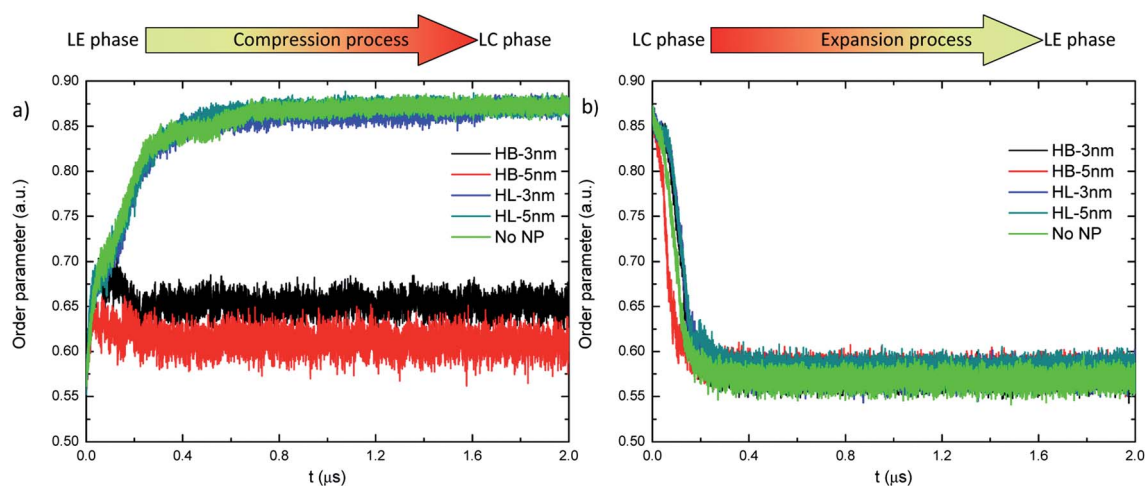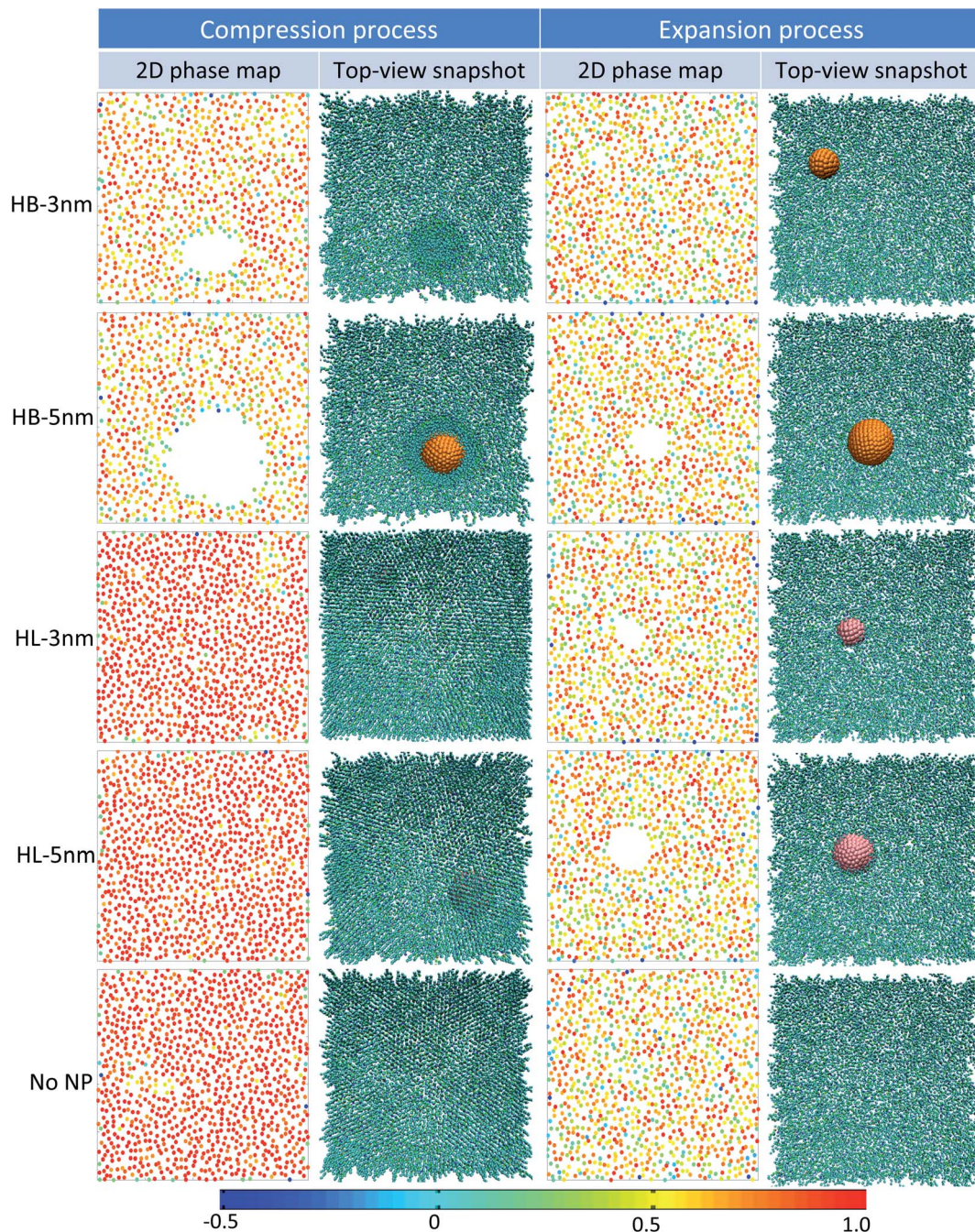

Fig. 3 Time evolution of order parameter of DPPC monolayer for all the simulation systems both in the compression (a) and the expansion (b) processes. Hydrophobic NP tends to inhibit the normal phase transition of DPPC monolayer during the compression process, while hydrophilic NP shows little or no effects on this transition of DPPC monolayer.

Fig. 4 Two-dimensional (2D) phase maps and top-view snapshots for all the simulation systems at $t = 0.8$ μs. The left two columns are for compression process and the right two for expansion process. The points in the 2D phase maps represent the interfacial DPPC molecules at the air–water interface and are colored according to the values of order parameter of the relative DPPC molecules. According to the color bar at the bottom, the redder color represents more order orientation of the interfacial DPPC molecules (more LC phase), and the bluer color represents more disorder orientation of the interfacial DPPC molecules (more LE phase). The blank regions of the map correspond to the situations that the large structural disruption is induced by NPs and the DPPC monolayer is embedded with NPs, which are further described in Fig. S2.† The color for the snapshots are the same as Fig. 1.

mechanics and further destabilize the interface structure of alveolus.[16–21] In our simulations, we found that large structural disruptions of DPPC monolayer are always accompanied by normal phase transition inhibition of interfacial DPPC molecules. And only hydrophobic NPs caused large structural disruptions and inhibited the normal phase transition of the

interfacial DPPC molecules. Hydrophilic NPs show excellent penetration ability and little structural disruptions to DPPC monolayer. Therefore, hydrophilic NPs are most suitable for respiratory drug delivery carriers. Along this line, surface modification of hydrophobic NPs with hydrophilic moieties, such as PEGylation, may help improve particle penetration

across the DPPC monolayer,[41] which will be studied in the next section.

Effects of hydrophilic modifications on interaction between hydrophobic NPs and the DPPC monolayer

Our simulation results showed that hydrophobic NPs tend to induce large structural disruption and inhibit the normal phase transition of the DPPC monolayer during the compression process, which suggests a potential side effect when using hydrophobic NPs for pulmonary delivery. Hence, we perform additional simulations to study the translocation ability of the hydrophobic NPs with hydrophilic surface modifications. We studied two widely used surface modification methods: non-covalent coating with DPPC molecules and covalent coating with PEG.[41]

For the non-covalent method, we firstly perform self-assembly simulation of a mixture of NP, DPPC and water molecules (here we use DPPC as a surfactant to obtain NP–surfactant complex because this will not change the composition of the DPPC monolayer with the interactions of NP–surfactant complex). Due to hydrophobic interactions, DPPC molecules can spontaneously adsorb onto the NP to form the complex with the hydrophilic head-group of DPPC exposing on the surface (Fig. 5a). After a pre-equilibrium simulation of the complex in the vacuum, the complex is placed near the DPPC monolayer for compression and expansion simulation to model the interactions between the inhaled complex and PS during respiratory process. The complex interacts with the DPPC monolayer to firstly form a local DPPC bilayer with NP embedded in it, and then the DPPC monolayer collapses quickly during the further compression process. The collapsed conformation consists of a "fold" structure with NP and an aggregate of DPPC molecules embedded in it (Fig. 5).[20] And the source of the aggregate absolutely comes from the NP–DPPC complex.

The above results point to a conclusion that the DPPC-coated NP obtained using the non-covalent method cannot effectively promote the translocation ability of the hydrophobic NP and reduce its potential side effects.

The inefficacy of DPPC-coated NP in penetrating the DPPC monolayer may be ascribed to the free amphiphilic molecules (DPPC) on its surface, which can easily flip-flop to form local bilayer structure and further promote the formation of large structural disruptions. In order to validate this hypothesis, we further probe the interactions between a DPPC liposome (i.e., closed DPPC bilayers self-assembled via non-covalent interactions) and a DPPC monolayer during the compression and expansion processes (Fig. 6). Results show DPPC molecules in the liposome can easily flip-flop to keep their hydrophobic tails facing the gas phase (also see Fig. S5†), and further induce large structural disruptions of the DPPC monolayer during the compression process and promote pore formation of the DPPC monolayer during the expansion process. These results are consistence with the simulations proposed by Baoukina et al.[42] for the interactions between the lipid bilayer aggregate in the vacuum and the lipid monolayer. Hence, the drug carrier systems using amphiphilic molecules (e.g., DPPC) as building block via non-covalent interactions may not be a good choice for respiratory therapy.

For the covalent method, we choose the commonly used PEGylation. Poly-(ethylene glycol) (PEG) has broad applications in biomedical formulations because of its favorable properties, such as low toxicity, biocompatibility, and ease of excretion.[43] In order to compare with the DPPC-coated NP, we used PEG9, which has a similar length to the DPPC molecule. The force field for the PEG has recently been developed and is compatible with the Martini force field used for all our simulations.[44,45] Using the similar simulation procedure as the DPPC-coated NP, we found that PEGylated NP can easily penetrate into the aqueous phase without provoking large structural disruption both in the compression and expansion processes (Fig. 5b). In other words,
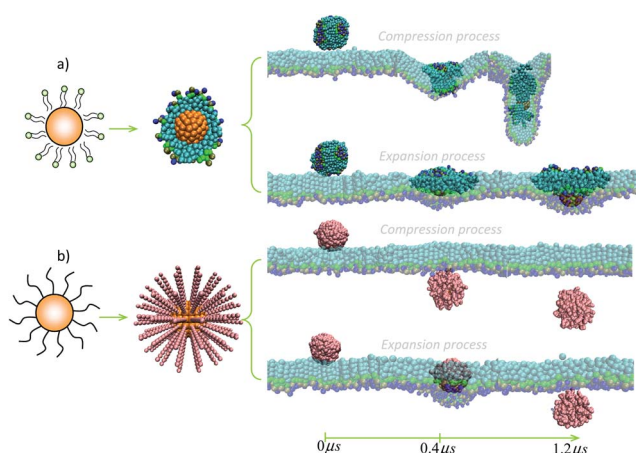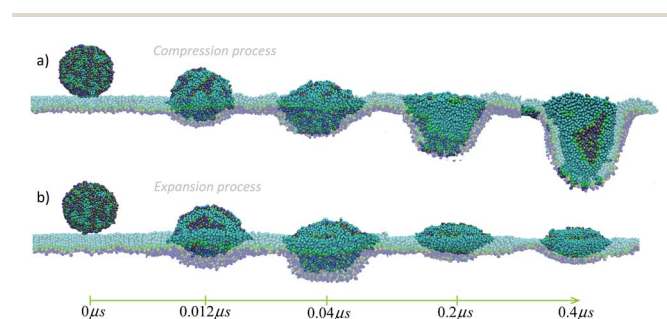

Fig. 5 The interactions between DPPC-coated (a) or PEGylated (b) hydrophobic NP and the DPPC monolayer during the compression and expansion processes. PEGylated hydrophobic NP can easily penetrate the DPPC monolayer both in compression and expansion process. However, DPPC-coated hydrophobic NP not only cannot penetrate the DPPC monolayer, but also induce collapse of the DPPC monolayer. Water molecules are not shown for clarity.

Fig. 6 The snapshots for the interaction of a DPPC liposome (d = 12 nm) with the DPPC monolayer during the compression (a) and expansion (b) processes. The morphology of the liposome experiences severe changes during its interactions with the DPPC monolayer and is trapped by the DPPC monolayer. The liposome causes a large structural disruption of the DPPC monolayer during the compression process and promotes pore formation of the DPPC monolayer during the expansion process (Fig. S4†). Water molecules are not shown for clarity.

PEGylated modification of hydrophobic NP may provide an effective way to promote the applicability of hydrophobic NPs as drug carriers in the respiratory therapy.

Conclusion

Pulmonary delivery using NPs as a drug carrier shows significant promises in respiratory therapy. It is critical to study the effects of NP on the pulmonary surfactant in order to promote its safer biomedical applications. Hence, we probe the interactions between NPs and the DPPC monolayer (as a simple model pulmonary surfactant) on molecular level using coarsegrained molecular dynamics simulations. As shown in Scheme 1, hydrophilic NP shows obvious advantages in translocation into the aqueous phase with little influence on the DPPC monolayer. However, hydrophobic NP tends to disrupt the DPPC monolayer and inhibit the normal phase transition during the compression process. Considering the hydrophobic NP's potential side effect, we try two hydrophilic treatments to reduce the side effect. Results show that the inhaled DPPC-coated NP can easily absorb onto the DPPC monolayer, form local DPPC bilayer with NP embedded in it, and further induce collapse of the DPPC monolayer during the compression process. However, PEGylated NP can penetrate into the aqueous phase with little influence on the structure and properties of the DPPC monolayer. Our results may glean insights for designing proper drug carrier systems for respiratory therapy and help evaluate NP's side effects on pulmonary surfactant.

Conflict of interest

The authors declare no competing financial interest.
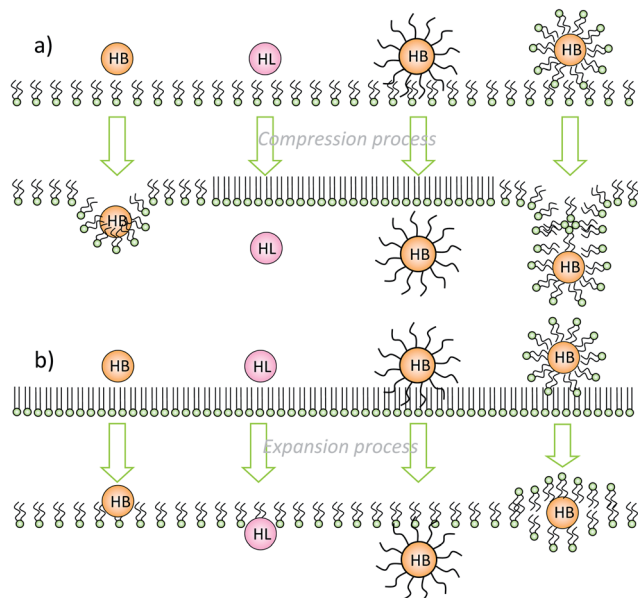
Scheme 1 Summary of the interactions between NPs (hydrophobic NP, hydrophilic NP, PEGylated hydrophobic NP, DPPC-coated hydrophobic NP) and the DPPC monolayer.

Notes and references

1 A. Weia, J. G. Mehtalaa and A. K. Patri, Challenges and opportunities in the advancement of nanomedicines, *J. Controlled Release*, 2012, **164**, 236–246.

2 Y. Wang, B. Yan and L. Chen, SERS Tags: Novel Optical Nanoprobes for Bioanalysis, *Chem. Rev.*, 2013, **113**, 1391–1428.

3 K. Saha, S. S. Agasti, C. Kim, X. Li and V. M. Rotello, Gold Nanoparticles in Chemical and Biological Sensing, *Chem. Rev.*, 2012, **112**, 2739–2779.

4 S. Muro, Challenges in design and characterization of ligand-targeted drug delivery systems, *J. Controlled Release*, 2012, **164**, 125–137.

5 T. L. Doane and C. Burda, The unique role of nanoparticles in nanomedicine: imaging, drug delivery and therapy, *Chem. Soc. Rev.*, 2012, **41**, 2885–2911.

6 J. Shi, A. R. Votruba, O. C. Farokhzad and R. Langer, Nanotechnology in Drug Delivery and Tissue Engineering: From Discovery to Applications, *Nano Lett.*, 2010, **10**, 3223–3230.

7 A. K. Sachan, R. K. Harishchandra, C. Bantz, M. Maskos, R. Reichelt, H. J. Galla, H. S. Choi, Y. Ashitate, J. H. Lee, S. H. Kim, A. Matsui, N. Insin, M. G. Bawendi, M. Semmler-Behnke, J. V. Frangioni and A. Tsuda, Rapid translocation of nanoparticles from the lung airspaces to the body, *Nat. Biotechnol.*, 2010, **28**, 1300–1303.

8 K. Donaldson, A. Schinwald, F. Murphy, W. S. Cho, R. Duffin, L. Tran and C. Poland, The Biologically Effective Dose in Inhalation Nanotoxicology, *Acc. Chem. Res.*, 2013, **46**, 723–732.

9 C. Y. Dombu and D. Betbeder, Airway delivery of peptides and proteins using nanoparticles, *Biomaterials*, 2013, **34**, 516–525.

10 D. K. Sung, W. H. Kong, K. Park, J. H. Kim, M. Y. Kim, H. Kim and S. K. Hahn, Noncovalenly PEGylated CTGF siRNA/ PDMAEMA complex for pulmonary treatment of bleomycin-induced lung fibrosis, *Biomaterials*, 2013, **34**, 1261–1269.

11 P. Wanakule, G. W. Liu, A. T. Fleury and K. Roy, Nano-inside-micro: Disease-responsive microgels with encapsulated nanoparticles for intracellular drug delivery to the deep lung, *J. Controlled Release*, 2012, **162**, 429–437.

12 C. Mühlfeld, B. Rothen-Rutishauser, F. Blank, D. Vanhecke, M. Ochs and P. Gehr, Interactions of nanoparticles with pulmonary structures and cellular responses, *Am. J. Physiol.: Lung Cell. Mol. Physiol*, 2008, **294**, L817–L829.

13 J. W. Card, D. C. Zeldin, J. C. Bonner and E. R. Nestmann, Pulmonary applications and toxicity of engineered nanoparticles, *Am. J. Physiol.: Lung Cell. Mol. Physiol*, 2008, **295**, L400–L411.

14 Y. Y. Zuo, R. A. W. Veldhuizen, A. W. Neumann, N. O. Petersen and F. Possmayer, Current perspectives in pulmonary surfactant-Inhibition, enhancement and evaluation, *Biochim. Biophys. Acta, Biomembr.*, 2008, **1778**, 1947–1977.

15 C. B. Daniels and S. Orgeig, Pulmonary Surfactant: The Key to the Evolution of Air Breathing, *Physiology*, 2003, **18**, 151–157.

16 J. M. Crane, G. Putz and S. B. Hall, Persistence of Phase Coexistence in Disaturated Phosphatidylcholine Monolayers at High Surface Pressures, *Biophys. J.*, 1999, **77**, 3134–3143.

17 C. Casals and O. Cañadas, Role of lipid ordered/disordered phase coexistence in pulmonary surfactant function, *Biochim. Biophys. Acta, Biomembr.*, 2012, **1818**, 2550–2562.

18 H. Zhang, Q. H. Fan, Y. E. Wang, C. R. Neal and Y. Y. Zuo, Comparative study of clinical pulmonary surfactants using atomicforce microscopy, *Biochim. Biophys. Acta, Biomembr.*, 2011, **1808**, 1832–1842.

19 S. Baoukina, L. Monticelli, S. J. Marrink and D. P. Tieleman, Pressure-Area Isotherm of a Lipid Monolayer from Molecular Dynamics Simulations, *Langmuir*, 2007, **23**, 12617–12623.

20 S. Baoukina, L. Monticelli, H. J. Risselada, S. J. Marrink and D. P. Tieleman, The molecular mechanism of lipid monolayer collapse, *Proc. Natl. Acad. Sci. U. S. A.*, 2008, **105**, 10803–10808.

21 S. Baoukina, E. Mendez-Villuendas and D. P. Tieleman, Molecular View of Phase Coexistence in Lipid Monolayers, *J. Am. Chem. Soc.*, 2012, **134**, 17543–17553.

22 J. Perez-Gil and T. E. Weaver, Pulmonary Surfactant Pathophysiology: Current Models and Open Questions, *Physiology*, 2010, **25**, 132–141.

23 M. S. Bakshi, L. Zhao, R. Smith, F. Possmayer and N. O. Petersen, Metal Nanoparticle Pollutants Interfere with Pulmonary Surfactant Function In Vitro, *Biophys. J.*, 2008, **94**, 855–868.

24 R. K. Harishchandra, M. Saleem and H. J. Galla, Nanoparticle interaction with model lung surfactant monolayers, *J. R. Soc., Interface*, 2010, **7**, S15–S26.

25 S. Choe, R. Chang, J. Jeon and A. Violi, Molecular Dynamics Simulation Study of a Pulmonary Surfactant Film Interacting with a Carbonaceous Nanoparticle, *Biophys. J.*, 2008, **95**, 4102–4114.

26 Q. H. Fan, Y. E. Wang, X. X. Zhao, J. S. C. Loo and Y. Y. Zuo, Adverse Biophysical Effects of Hydroxyapatite Nanoparticles on Natural Pulmonary Surfactant, *ACS Nano*, 2011, **5**, 6410–6416.

27 E. López-Rodríguez, O. L. Ospina, M. Echaide, H. W. Taeusch and J. Pérez-Gil, Exposure to Polymers Reverses Inhibition of Pulmonary Surfactant by Serum, Meconium, or Cholesterol in the Captive Bubble Surfactometer, *Biophys. J.*, 2012, **103**, 1451–1459.

28 X. B. Lin, Y. Li and N. Gu, Molecular dynamics simulations of the interactions of charge-neutral PAMAM dendrimers with pulmonary surfactant, *Soft Matter*, 2011, **7**, 3882–3888.

29 S. J. Marrink, H. J. Risselada, S. Yefimov, D. P. Tieleman and A. H. de Vries, The MARTINI Force Field: Coarse Grained Model for Biomolecular Simulations, *J. Phys. Chem. B*, 2007, **111**, 7812–7824.

30 L. Monticelli, S. K. Kandasamy, X. Periole, R. G. Larson, D. P. Tieleman and S. J. Marrink, The MARTINI Coarse-Grained Force Field: Extension to Proteins, *J. Chem. Theory Comput.*, 2008, **4**, 819–834.

31 L. Y. Lu and G. A. Voth, Systematic Coarse-graining of a Multicomponent Lipid Bilayer, *J. Phys. Chem. B*, 2009, **113**, 1501–1510.

32 Z. J. Wang and M. Deserno, A Systematically Coarse-Grained Solvent-Free Model for Quantitative Phospholipid Bilayer Simulations, *J. Phys. Chem. B*, 2010, **114**, 11207–11220.

33 X. B. Lin, C. L. Wang, M. Wang, K. Fang and N. Gu, Computer Simulation of the Effects of Nanoparticles' Adsorption on the Properties of Supported Lipid Bilayer, *J. Phys. Chem. C*, 2012, **116**, 17960–17968.

34 H. J. C. Berendsen, J. P. M. Postma, W. F. van Gunsteren, A. DiNola and J. R. Haak, Molecular dynamics with coupling to an external bath, *J. Chem. Phys.*, 1984, **81**, 3684–3690.

35 W. Humphrey, A. Dalke and K. Schulten, VMD: Visual Molecular Dynamics, *J. Mol. Graphics*, 1996, **14**, 33–38.

36 B. Hess, C. Kutzner, D. van der Spoel and E. Lindahl, GROMACS 4: Algorithms for Highly Efficient, Load-Balanced, and Scalable Molecular Simulation, *J. Chem. Theory Comput.*, 2008, **4**, 435–447.

37 C. Bernardini, S. D. Stoyanov, L. N. Arnaudov and M. A. C. Stuart, Colloids in Flatland: a perspective on 2D phase-separated systems, characterisation methods, and lineactant design, *Chem. Soc. Rev.*, 2013, **42**, 2100–2129.

38 C. Chiu, W. Shinoda, R. H. DeVanec and S. O. Nielsen, Effects of spherical fullerene nanoparticles on a dipalmitoyl phosphatidylcholine lipid monolayer: a coarse grain molecular dynamics approach, *Soft Matter*, 2012, **8**, 9610–9616.

39 C. C. Kuo, A. T. Kodama, T. Boatwright and M. Dennin, Particle Size Effects on Collapse in Monolayers, *Langmuir*, 2012, **28**, 13976–13983.

40 S. Tatur and A. Badia, Influence of Hydrophobic Alkylated Gold Nanoparticles on the Phase Behavior of Monolayers of DPPC and Clinical Lung Surfactant, *Langmuir*, 2012, **28**, 628–639.

41 S. T. Kim, K. Saha, C. Kim and V. M. Rotello, The Role of Surface Functionality in Determining Nanoparticle Cytotoxicity, *Acc. Chem. Res.*, 2013, **46**, 681–691.

42 S. Baoukina, L. Monticelli, M. Amrein and D. P. Tieleman, The Molecular Mechanism of Monolayer-Bilayer Transformations of Lung Surfactant from Molecular Dynamics Simulations, *Biophys. J.*, 2007, **93**, 3775–3782.

43 F. M. Veronese, Peptide and protein PEGylation: a review of problems and solutions, *Biomaterials*, 2001, **22**, 405–417.

44 H. Lee, A. H. de Vries, S. J. Marrink and R. W. Pastor, A Coarse-Grained Model for Polyethylene Oxide and Polyethylene Glycol: Conformation and Hydrodynamics, *J. Phys. Chem. B*, 2009, **113**, 13186–13194.

45 H. Lee and R. W. Pastor, Coarse-Grained Model for PEGylated Lipids: Effect of PEGylation on the Size and Shape of Self-Assembled Structures, *J. Phys. Chem. B*, 2011, **115**, 7830–7837.